

Dielectric-Loaded Lens Applicator for Microwave Hyperthermia

Yoshio Nikawa, *Member, IEEE*, and Fumiaki Okada, *Senior Member, IEEE*

Abstract—One characteristic desirable in the hyperthermia treatment of cancer is the ability to achieve deep, localized microwave heating of the human body. A newly developed lens applicator has achieved this through the integration of a waveguide partially filled with dielectric. The heating pattern of the applicator can be controlled by varying the size of the dielectric material. Heating experiments on a model simulating human muscle have shown that an applicator with an aperture of $150 \times 100 \text{ mm}^2$ achieves a maximum heating depth of over 80 mm, results that are well in line with the deep, localized heating required for hyperthermia.

I. INTRODUCTION

MICROWAVE technology has been viewed as a potential source for achieving deep, localized hyperthermia within the human body [1]–[3]. However, a major difficulty has been the skin depth of a few centimeters of human muscle in the microwave region. Actually, the skin depth of human muscle at 430 MHz is at most 40 mm. Although multiapplicators have appeared to be the best approach for overcoming this problem and achieving deep heating, they have proven cumbersome to set up [4], [5].

The authors previously developed lens applicators [6], [7], containing metal plates, which radiate focused microwaves for deep penetration into a lossy medium. Unfortunately, the structures of these lenses were somewhat complicated.

This paper describes a new lens applicator which can concentrate the *E*-plane field in a lossy medium and is constructed of an easily fabricated, dielectric-filled waveguide. Since the microwave field distribution on the aperture can be varied by using different sizes of dielectric material, the heating pattern inside the medium can be changed, allowing the configuration of a compact applicator that can heat portions deeper within the human body.

II. APPLICATOR DESIGN

Fig. 1 shows an applicator with a dielectric slab centered in a water-filled waveguide. Fig. 2 shows the aperture of the applicator and its parameters. A fixed rectangular coordinate system located on the aperture of the applicator is also shown in Fig. 2. The phase constant of

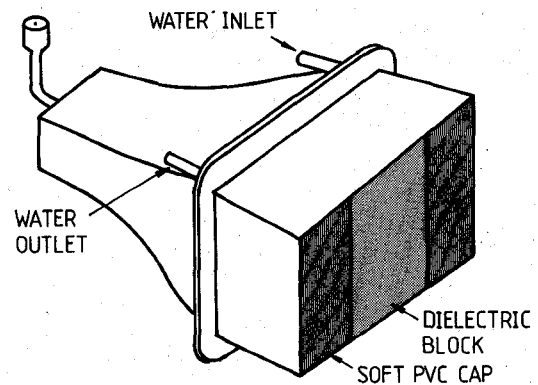


Fig. 1. Dielectric-loaded lens applicator.

the waveguide filled with dielectric can be calculated as [8]

$$\frac{\beta}{k_1} = \sqrt{1 + \frac{\epsilon_2 - \epsilon_1}{\epsilon_1} \left(\frac{d}{a} + \frac{1}{\pi} \sin \frac{\pi d}{a} \right) - \left(\frac{\pi}{k_1 a} \right)^2} \quad (1)$$

where k_1 is the propagation constant of water and β is the phase constant in the waveguide; ϵ_1 and ϵ_2 are the dielectric constants of water and the center dielectric material, respectively. Polyethylene ($\epsilon_2 = 2.3$) is taken to be the center dielectric material. Fig. 3 shows the results of β/k_1 as a function of a/λ_1 . The result demonstrated the propagation constant inside the dielectric-filled waveguide to be smaller than that of the normal water-loaded waveguide. The size of aperture a was decided using Fig. 3. The aperture size of the applicator is $150 \times 100 \text{ mm}^2$ and is operated at 430 MHz. The applicator is fed by an easy-to-handle magnetic field coupling device. The reflection coefficient of the applicator is a minimum (-19.3 dB) at 430 MHz.

III. EXPERIMENT

A. Electric Field Distribution

Experiments measuring the electric field distribution on the aperture of an applicator used an 0.4% NaCl solution as the electrical equivalent model of human muscle [9], [10]. Dielectric materials of various width, d , were prepared to set inside the applicator. The experimental setup for measuring the electric field is shown in Fig. 4. In the experiment, the applicator is set inside a

Manuscript received August 10, 1990; revised February 13, 1991.

The authors are with the Department of Electrical Engineering, National Defense Academy, 1-10-20 Hashirimizu, Yokosuka 239, Japan. IEEE Log Number 9100137.

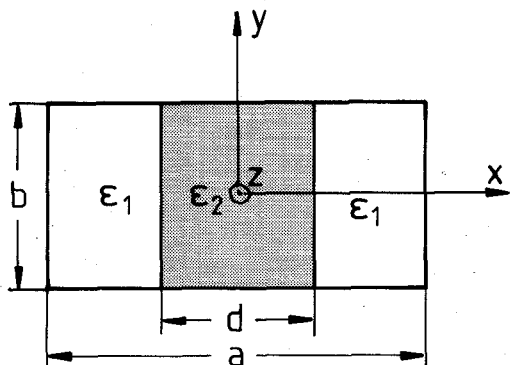


Fig. 2. The aperture of the applicator.

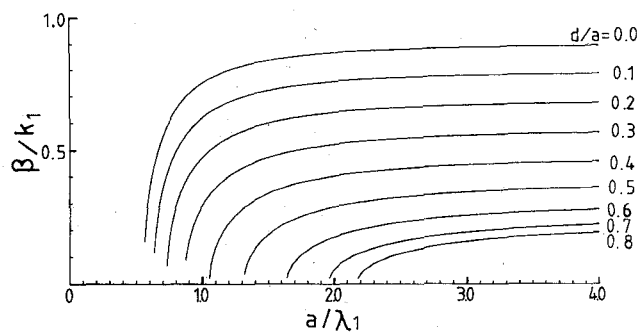


Fig. 3. Phase constant for a rectangular waveguide of a loaded centered dielectric.

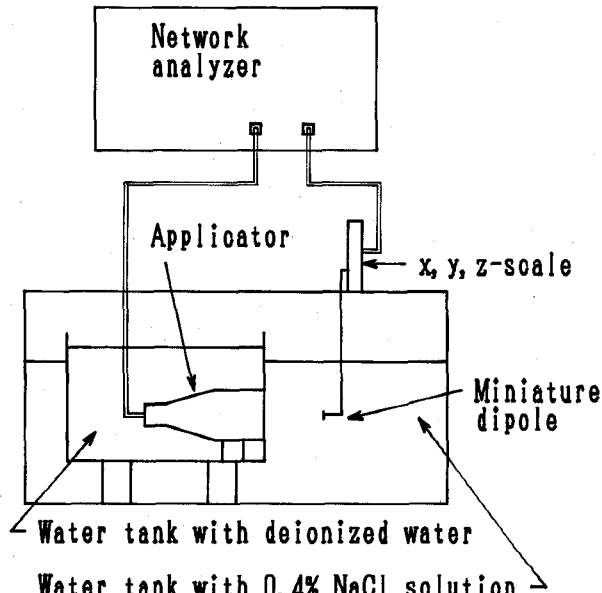


Fig. 4. Experimental setup for measuring electric field distribution from the aperture of an applicator.

Plexiglas tank filled with deionized water, which itself is set in a larger tank, measuring $1.0 \text{ m} \times 1.0 \text{ m} \times 0.5 \text{ m}$, which is filled with 0.4% NaCl solution. The radiated microwave from the aperture of the applicator is detected by a miniature dipole probe of length 15 mm that can move in the x , y , and z directions. The dipole probe is small enough and the medium is very lossy; therefore the

probe does not disturb the aperture field of the applicator. The radiated microwave is measured by a network analyzer (HP-8505A). We have considered only the y component of the electric field because the x and z components of the field turn out to be negligible [6].

Two-dimensional measurements of the electric field with the phase distribution in the 0.4% NaCl solution were performed for various sizes of dielectric materials. The results of the measurements for $d = 45 \text{ mm}$, 75 mm , and 90 mm are shown in Figs. 5, 6, and 7. Figs. 5(a), 6(a), and 7(a) show the electric field distributions on a contour map that is normalized on the origin of the axes with a contour interval of 1 dB. Figs. 5(b), 6(b), and 7(b) show phase distributions on a contour map having a contour interval of 10° . These figures indicate that the focusing effect can be varied by using different sizes of dielectric materials.

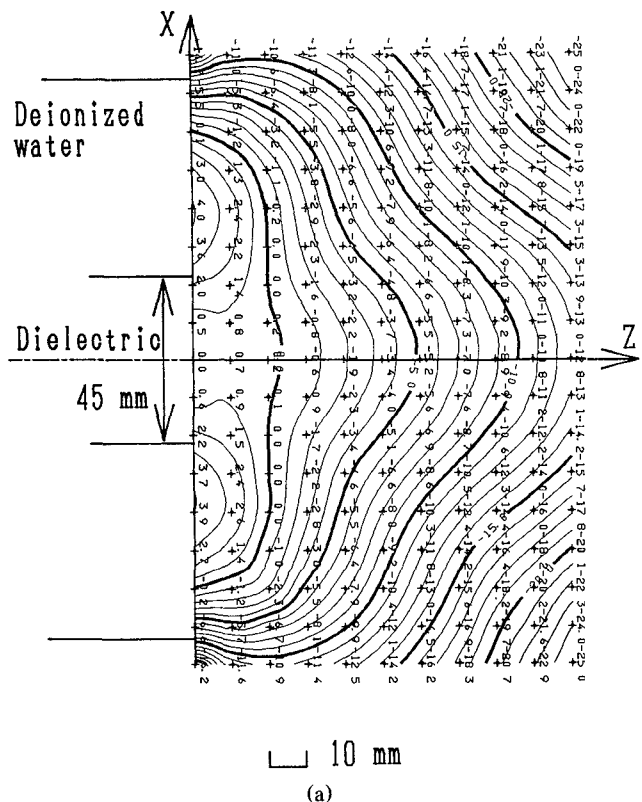
As shown in Figs. 5(b), 6(b), and 7(b), the leading phase of the side portion of the applicator results in an obvious focusing of the radiated electric field. The lead phase angle is about 60° for a dielectric material of $d = 75 \text{ mm}$. In the case of $d = 75 \text{ mm}$ and 90 mm , the converging effect continues to increase despite an increase of z ; this is in contrast to the case of $d = 45 \text{ mm}$.

The amplitude distribution on the aperture also affects the convergence of the field: the stronger the amplitude of the side portion of the applicator, the stronger the focusing effect of the radiated electric field, as shown in Figs. 5(a), 6(a), and 7(a).

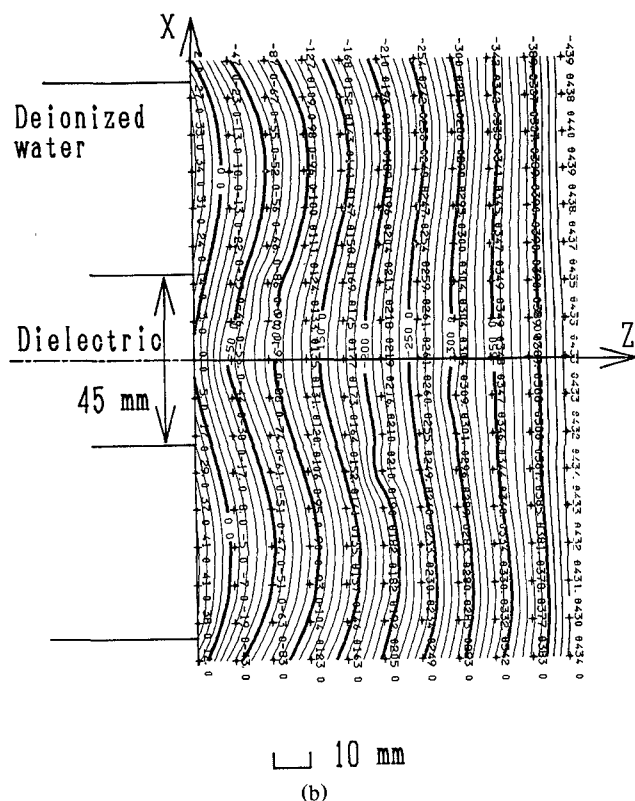
Fig. 8 shows the electric field distribution as a function of depth for four different values of d plotted on the z axis. The electric field is normalized on the origin. As can be seen from the figure, a center dielectric of $d = 90 \text{ mm}$ exhibits a maximum relative electric field of +3 dB, or 200% of the specific absorption rate (SAR) normalized at the origin. The same dielectric exhibits a relative electric field of -3 dB, or 50% of SAR exhibited at the origin, where z measures 80 mm. A center dielectric of $d = 45 \text{ mm}$ exhibits a maximum relative electric field of +0.8 dB, or 120% of SAR normalized at the origin. The same dielectric exhibits a relative electric field of -3 dB, or 50% of SAR exhibited at the origin, where z measures 45 mm.

B. Muscle Model Heating

Heating experiments were performed on a model simulating human muscle (0.4% NaCl, 0.02% NaN₃, and 4% agar). Fig. 9 shows the temperature distribution on the $x-z$ plane after an exposure of 430 MHz radiation using the $d = 75 \text{ mm}$ applicator. The rate of temperature elevation where $z = 25 \text{ mm}$ was controlled at 1°C per minute. And the surface of the model was cooled at the initial temperature of the model (20.0°C) by flowing water. In this case, radiation was applied to the model by the applicator through a 2 mm cooling water layer. Results showed that the heating depth for a temperature of $\Delta T_{\max}/2$ is as close as 60 mm.

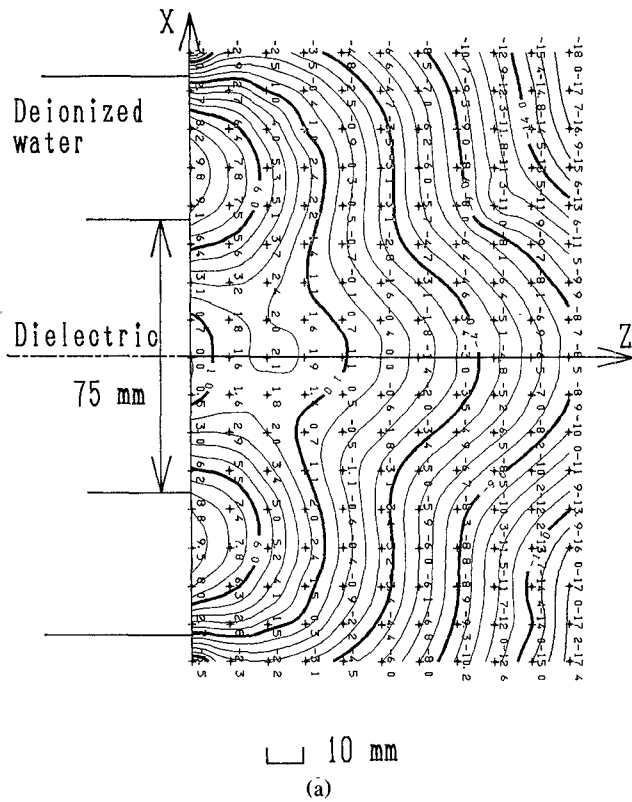


(a)

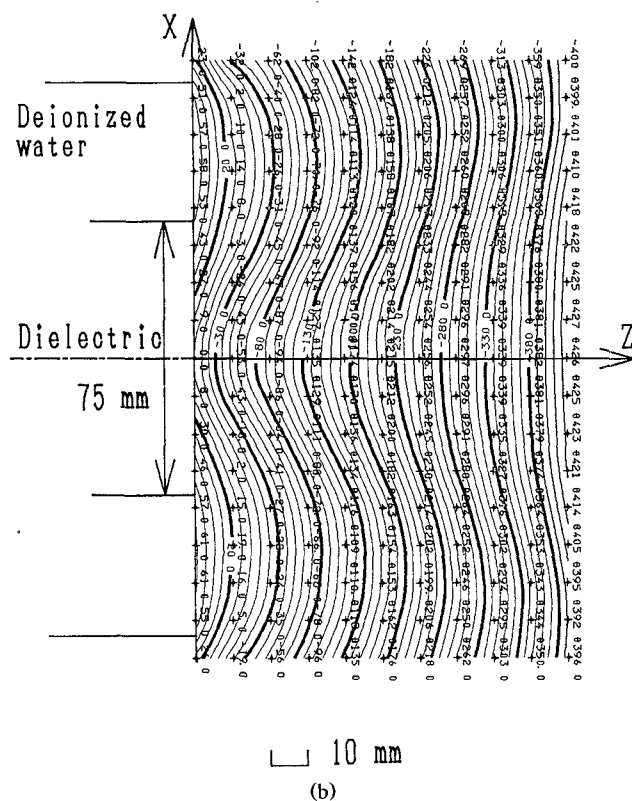


(b)

Fig. 5. Two-dimensional distribution of the electric field ($d = 45$ mm):
(a) amplitude distribution; (b) phase distribution.



(a)



(b)

Fig. 6. Two-dimensional distribution of the electric field ($d = 75$ mm):
(a) amplitude distribution; (b) phase distribution.

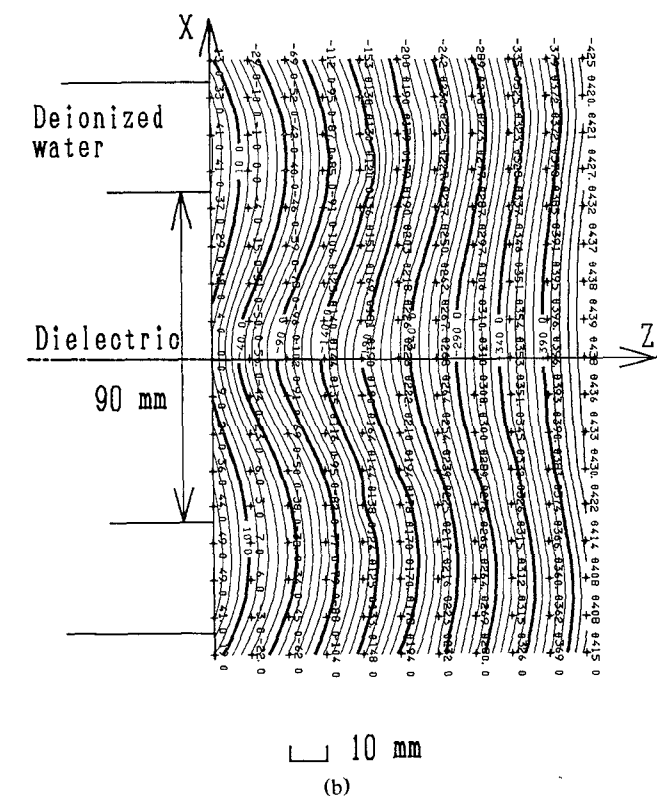
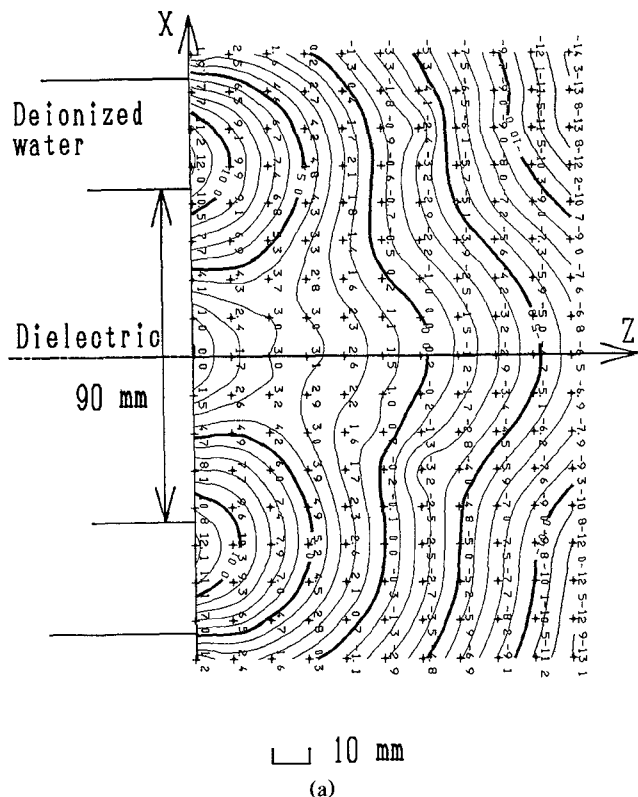


Fig. 7. Two-dimensional distribution of the electric field ($d = 90$ mm): (a) amplitude distribution; (b) phase distribution.

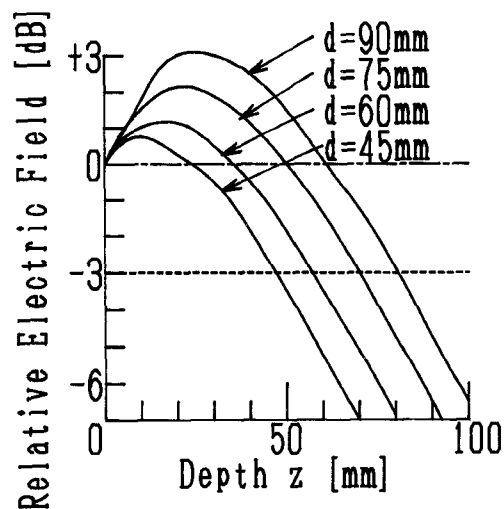


Fig. 8. Electric field distribution from the aperture of the applicator in direct contact with simulated human muscle.

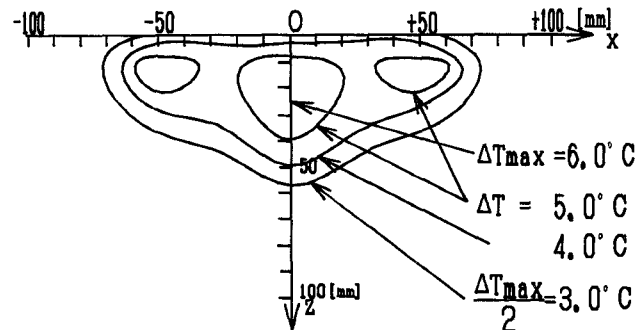


Fig. 9. Two-dimensional temperature elevation distribution in the simulated muscle heated by an applicator of $d = 75$ mm.

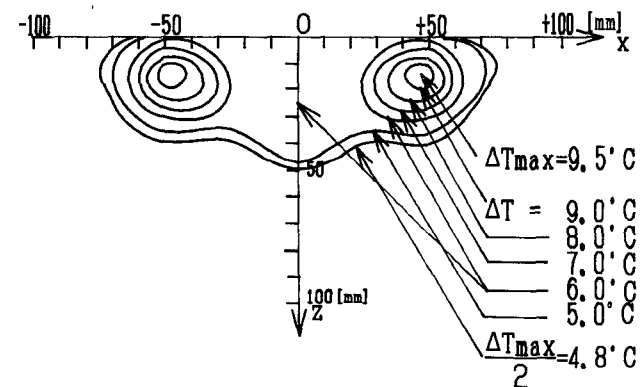


Fig. 10. Two-dimensional temperature elevation distribution in the simulated muscle heated by an applicator of $d = 90$ mm.

Fig. 10 shows the temperature distribution on the $x-z$ plane after an exposure of 430 MHz radiation using the $d = 90$ mm applicator. The rate of temperature elevation where $z = 25$ mm was controlled at 1°C per minute. Results showed that the heating depth for a temperature of $\Delta T_{\text{max}}/2$ is around 50 mm. When $d = 90$ mm is used, the electric field in the side portion of the applicator becomes strong, resulting in strong heating at the side

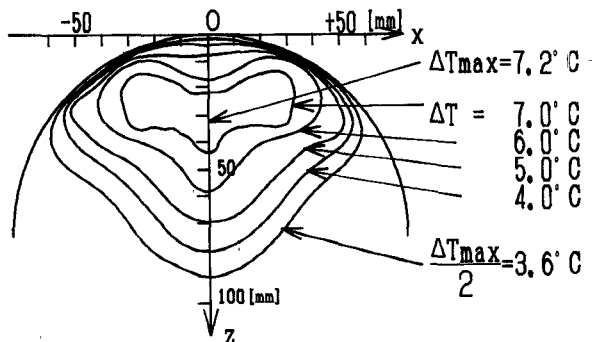


Fig. 11. Two-dimensional temperature elevation distribution in cylindrically shaped simulated muscle with a diameter of 150 mm heated by an applicator of $d = 90$ mm.

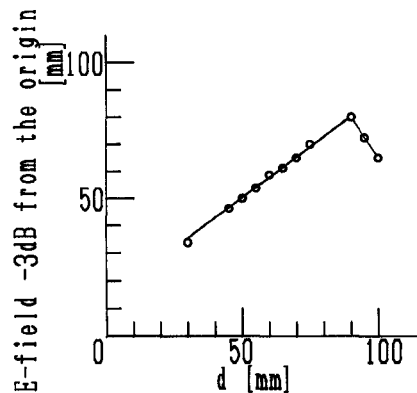


Fig. 12. Electric field decreases to -3 dB from the origin versus width of the dielectric material.

portion. As is shown in Fig. 10, the temperature where $(x, y, z) = (\pm 50 \text{ mm}, 0 \text{ mm}, 15 \text{ mm})$ was the maximum and was 3.5°C higher than that where $(x, y, z) = (0 \text{ mm}, 0 \text{ mm}, 25 \text{ mm})$.

Fig. 11 shows the temperature distribution on the $x-z$ plane after an exposure of 430 MHz radiation on a 150-mm-diameter cylindrical model using an applicator of $d = 90$ mm. The gap between the cylindrical surface and the two sides of the applicator is filled with cooling water, preventing the temperature from rising in these areas. The temperature of $\Delta T_{\max}/2$ was achieved at a heating depth of 90 mm. These results confirm the electric field measurements.

IV. RESULTS

The results of two-dimensional electric field measurements proved that dielectric material of $d = 45$ mm achieved uniform heating in the x direction but not deep heating (see Fig. 5(a)). On the other hand, when dielectric material of $d = 90$ mm was used, even though surface cooling was required on both sides of the applicator aperture, heating was achieved at 90 mm.

The depth of the heating can be estimated from the electric field distribution along the z axis. The maximum heating depth is defined as the depth where the electric field decreases to -3 dB from the origin (where the SAR

decreases 50%) and is given as a function of d , as shown in Fig. 12. The heating depth increases in proportion to d up to 90 mm, which is below the cutoff region. At d greater than 90 mm, it decreases with increases in d above the cutoff region. Refer to Fig. 12 for optimum heating conditions at various locations of heating inside muscle tissue. The presence of a fat layer with a relative complex permittivity is $5.5 - j2.43$ (at 450 MHz) [11] and a skin depth over 200 mm will disturb the electric field radiated from the aperture. Nevertheless, the skin depth is very large and the heat generation in the fat layer is very low, so the depth of heating in the muscle may not be so reduced.

V. CONCLUSION

A 430 MHz lens applicator with an aperture size of $150 \times 100 \text{ mm}^2$ has been developed. The convergence effects of the electric field were observed and were dependent on the width of the dielectric material. The heating results of a model simulating human muscle show that the depth of heating where a temperature of $\Delta T_{\max}/2$ is achieved exceeds 80 mm and that when cylindrical models were used, the depth of heating was 90 mm. These results show that the heating depth can be increased by a factor of more than 2 over that obtained by conventional waveguide applicators, whose depth of heating is approximately 30 mm at this frequency. Furthermore, the relation between the width of the dielectric material and the maximum heating depth was clarified in its application to optimum heating. These results will be highly useful for deep, local hyperthermia treatment.

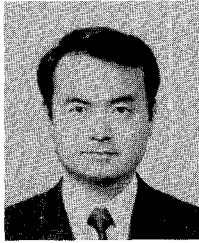
ACKNOWLEDGMENT

The authors wish to thank T. Mizuno, R. Kaneko, M. Kondoh, Y. Ashikawa, and Y. Hara of Tokimek Inc. for providing necessary materials and suggestions.

REFERENCES

- [1] F. Sterzer, R. W. Paglione, J. Mendecki, E. Friendenthal, and C. Botstein, "RF therapy for malignancy," *IEEE Spectrum*, vol. 17, pp. 32-37, Dec. 1980.
- [2] R. H. Johnson *et al.*, "New low-profile applicators for local heating of tissues," *IEEE Trans. Biomed. Eng.*, vol. BME-31, pp. 28-37, Jan. 1984.
- [3] G. Kantor, "Evaluation and survey of microwave and radio frequency applicators," *J. Microwave Power*, vol. 16, pp. 135-150, 1981.
- [4] P. F. Turner, "Regional hyperthermia with an annular phased array," *IEEE Trans. Biomed. Eng.*, vol. BME-31, pp. 106-114, Jan. 1984.
- [5] P. F. Turner, "Hyperthermia and inhomogeneous tissue effects using an annular phased array," *IEEE Trans. Microwave Theory Tech.*, vol. MTT-32, pp. 874-882, Aug. 1984.
- [6] Y. Nikawa, M. Kikuchi, and S. Mori, "Development and testing of a 2450-MHz lens applicator for localized microwave hyperthermia," *IEEE Trans. Microwave Theory Tech.*, vol. MTT-33, pp. 1212-1216, Nov. 1985.
- [7] Y. Nikawa, T. Katsumata, M. Kikuchi, and S. Mori, "An electric field converging applicator with heating pattern controller for microwave hyperthermia," *IEEE Trans. Microwave Theory Tech.*, vol. MTT-34, pp. 631-635, May 1986.

- [8] R. F. Harrington, *Time-Harmonic Electromagnetic Fields*. New York: McGraw-Hill, 1961, ch. 7.
- [9] A. Kumar, "Complex permittivity and microwave heating of pure water, tap water and salt solution," *Int. J. Electron.*, vol. 47, no. 6, pp. 531-536, 1979.
- [10] M. A. Stuchly and C. C. Stuchly, "Dielectric properties of biological substances—Tabulated," *J. Microwave Power*, vol. 15, pp. 19-26, 1980.
- [11] A. W. Guy and J. F. Lehmann, "On the determination of an optimum microwave diathermy frequency for a direct contact applicator," *IEEE Trans. Biomed. Eng.*, vol. BME-13, pp. 76-87, Apr. 1966.

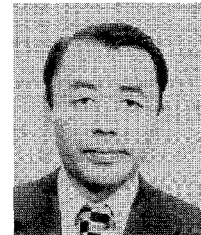


Yoshio Nikawa (M'88) was born in Tokyo, Japan, on March 30, 1958. He received the B.E., M.E., and Ph.D. degrees in electrical engineering from Keio University, Yokohama, Japan, in 1981, 1983, and 1986, respectively.

From April 1986 to July 1987 he was a Research Assistant at the National Defense Academy, Yokosuka, Japan. From July 1987 to July 1988 he was a Research Associate at the University of Texas at Austin. In July 1988 he returned to the National Defense Academy,

where he is now an Associate Professor in the Department of Electrical Engineering. He has worked on microwave devices and microwave applications. His current research interests are microwave measurements, applications, and EM wave heating techniques for hyperthermia and medical electronics.

Dr. Nikawa is a member of the IEICE of Japan, the Japan Society of Medical Electronics and Biological Engineering and the Japanese Society of Hyperthermic Oncology.



Fumiaki Okada (M'71-SM'79) was born in Tochigi, Japan, on December 14, 1927. He received the B.E., M.E. and Dr. Eng. degrees from Waseda University, Tokyo, Japan in 1951, 1954, and 1957, respectively.

He was with the Department of Electrical Engineering at the National Defense Academy, Yokosuka, Japan, as a Lecturer and an Associate Professor from 1957 to 1968. Since 1968 he has been a Professor there. His current research deals with microwave solid-state devices and measurements, especially microwave ferrite, and high-power microwave devices.

Dr. Okada is a member of the IMPI, the IEICE, and the ITE of Japan.